Control spiral wave dynamics using feedback signals from line detectors

Guoyong Yuan[1,2] [(a)], Aiguo Xu[3] , Guangrui Wang[3] and Shigang Chen[3]

[1] *Department of Physics,Hebei Normal University - Shijiazhuang,050016, China*
[2] *Hebei Advanced Thin Films Laboratory - Shijiazhuang,050016, China*
[3] *Institute of Applied Physics and Computational Mathematics- P. O. Box 8009, Beijing 100088,China*

arXiv:1004.0045v1 [cond-mat.stat-mech] 1 Apr 2010

PACS 05.45.-a – Nonlinear dynamics and chaos
PACS 05.65.+b – Self-organized systems
PACS 47.54.-r – Pattern selection; pattern formation

Abstract. - We numerically study trajectories of spiral-wave-cores in excitable systems modulated proportionally to the integral of the activity on the straight line, several or dozens of equi-spaced measuring points on the straight line, the double-line and the contour-line. We show the single-line feedback results in the drift of core center along a straight line being parallel to the detector. An interesting finding is that the drift location in y is a piecewise linear-increasing function of both the feedback line location and time delay. Similar trajectory occurs when replacing the feedback line with several or dozens of equi-spaced measuring points on the straight line. This allows to move the spiral core to the desired location along a chosen direction by measuring several or dozens of points. Under the double-line feedback, the shape of the tip trajectory representing the competition between the first and second feedback lines is determined by the distance of two lines. Various drift attractors in spiral wave controlled by square-shaped contour-line feedback are also investigated. A brief explanation is presented.

Introduction. – Spiral waves are typical examples of spatiotemporal patterns in macroscopic systems driven far from thermodynamic equilibrium. They exist extensively in excitable and self-oscillating media[1]. For example, cardiac muscle[2], platinum with oxidation of CO [3], liquid crystal subjected to electric or magnetic field[4],the slime mould dictyostelium discoideum[5] and reacting chemical systems[6]. The dynamics of spiral wave has attracted considerable interest, which is attributed not only to the characteristics of its nonlinearity and being far from equilibrium, but also to its extensive destructions/applications. For example, spiral waves and spatiotemporal chaos from repetitious breakup of spiral waves in cardiac muscle may be the leading mechanism of tachycardia and ventricular fibrillation[7]. Spiral waves in the brain are believed to be associated with epilepsy[8]. Therefore, how to control or eliminate spiral waves and spatiotemporal chaos is an interesting research topic[9-14].

Recently, much attention has been paid to the dynamics of spiral waves subjected to a feedback signal. The motions of spiral core have been studied under a number of different feedbacks. These feedbacks can be grouped into two classes, local feedback and non-local feedback. Local feedback is also referred to as one-channel feedback. It is performed according to the state at a single measuring point of the excitable system. Non-local feedback is performed according to states at more than one points, normally the mean state over a region. Under local feedback control the trajectory of spiral core is attracted to a series of limiting cycles centered on the measuring point[15-21]. If the motion on the innermost limit cycle is epicycloidal, then this limiting cycle is referred to as the entrainment attractor. Limiting cycles being further from the measuring point are referred to as resonance attractors. The radius of the attractor is dependent on the time delay. The most straightforward generalization of one-channel feedback is to monitor the states of system at two points and put in signals from both to determine the strength of the feedback signal[22-23].

It has been observed that two-channel feedback destroys the regular dynamics seen in one-channel feedback if the measuring points are sufficiently separated, and that several complex regimes appear when varying the distance

[(a)] g-y-y1975@sohu.com

between the two measuring point. In the other types of non-local feedback, the modulation is proportional to the integral of the activity in 2D excitable domains of different shapes[24-32]. The behaviors of attractors have been examined for circular, square, elliptical, triangle, pentagon and rhombus domains. When the domain size is significantly smaller than the wavelength of spiral wave, the spiral core trajectories are similar to those for local feedback. However, for larger domains, the attractors depend significantly on the size and shape of the domain.

In this letter we numerically study the behaviors of feedback control from several kinds of line detectors to compensate the lack of one-dimensional(1D) case between the zero-dimensional point and the 2D domains mentioned above. The measuring domain is one of the following cases, (i) a straight line, (ii)several or dozens of equi-spaced measuring points on the straight line , (iii)a double-line, (iv)a contour-line.

The mathematical model. – In our study the FizHugh-Nagumo(FHN) model[33-34] is used to describe the excitable media. The FHN model is a set of two-variable "reaction-diffusion" equations. This model is generic for excitable systems and can be applied to a variety of systems. It can reproduce many qualitative characteristics of electrical impulses along nerve and cardiac fibers, such as the existence of an excitation threshold, relative and absolute refractory periods, and the generation of pulse trains under the action of external currents. The FHN model with a line feedback reads

$$\frac{\partial u}{\partial t} = \frac{1}{\varepsilon}[-v - u(u-a)(u-1)] + \nabla^2 u + \frac{I}{\varepsilon} \quad (1)$$

$$\frac{\partial v}{\partial t} = -\gamma v + \beta u - \delta \quad (2)$$

where the variables $u(x, y, t)$ and $v(x, y, t)$ are the activator and inhibitor, respectively; ε is the time scale and named excitability parameter; a represents the threshold for excitation; γ, β and δ are parameters controlling the rest state and dynamics. Here, $a = 0.03$, $\gamma = 1.0$, $\delta = 0.0$,$\beta = 2.0$ and $\varepsilon = 0.004$. To perform the line feedback, the modulation signal $I(t)$ is computed as

$$I(t) = k_{fb}(B(t-\tau) - B_0) \quad (3)$$

where

$$B(t) = \frac{1}{L}\int_L u(x', y', t)ds' \quad (4)$$

Thus, the feedback signal is proportional to the integral value B of the first variable over the measuring line of length L taken with a time delay τ. The parameter k_{fb} is the feedback gain, and B_0 is the average value of $B(t)$ over one revolution of a spiral wave without feedback. In numerical simulations the system (1)-(2) is integrated by split operator method with the time step $\Delta t = 0.005$ t.u., the space step $h = 0.1$ s.u. and a 200×200 array. No-flux boundary conditions are used.

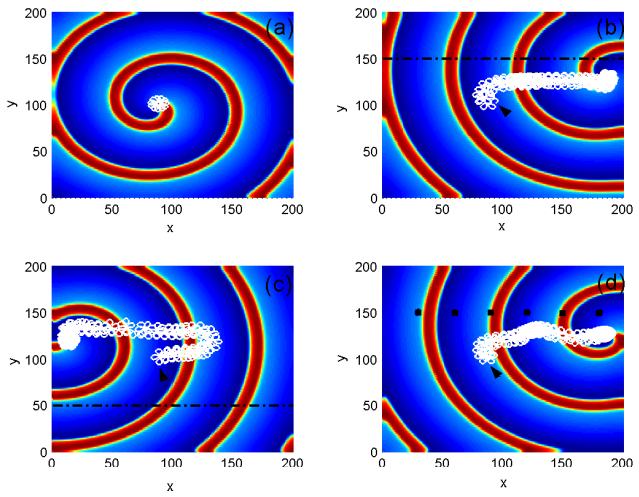

Fig. 1: (Color online) Trajectories of a spiral wave tip subjected to the feedback control shown in Eqs.(3) and (4) for different locations of the line. Fig. (a) is for the initial spiral wave and its tip before switching on the feedback control. The feedback lines are indicated by back dash-dotted line in (b) and (c). y_{fb}=150 in (b) and y_{fb}=50 in (c). Fig. (d) is for the trajectory of a spiral wave tip subjected to the feedback derived from six equi-spaced measuring points with y_{fb}=150. The spiral images are shown for the end of the trajectory in (b),(c) and (d). Here $k_{fb} = 0.05$, $\tau = 10$.

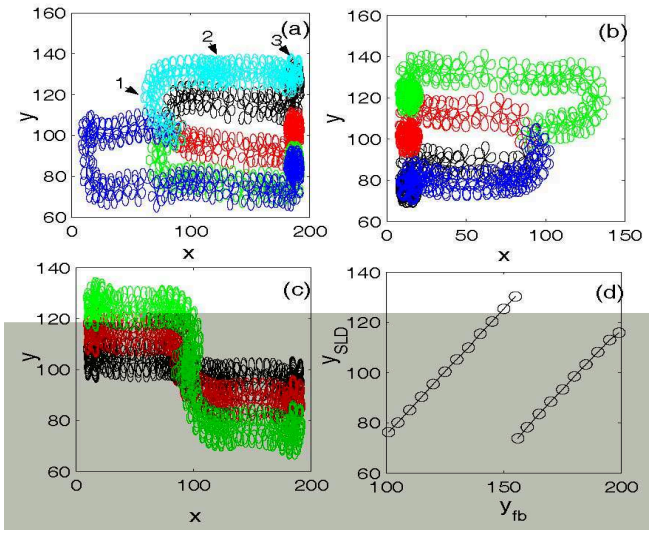

Fig. 2: (Color online)Trajectories of spiral wave tip under feedback control for different locations of the feedback line. In Fig. (a) the values of y_{fb} corresponding to the black, red, green, blue and cyan lines are 199, 175, 158, 156, and 155, respectively. In Fig. (b) the values of y_{fb} corresponding to the black, red, green, blue, lines are 5, 30, 50, 55, respectively. In Fig. (c) the values of y_{fb} corresponding to the left black, left red, left green, right black, right red, right green are 80, 90, 100, 120, 112, 101, respectively. Fig.(d) shows the location of the SLD y_{SLD} vs. that of the feedback line y_{fb}. Here the measuring line is parallel to the x-axis and has a length $L = 200$. k_{fb}=0.05 and $\tau = 10$.

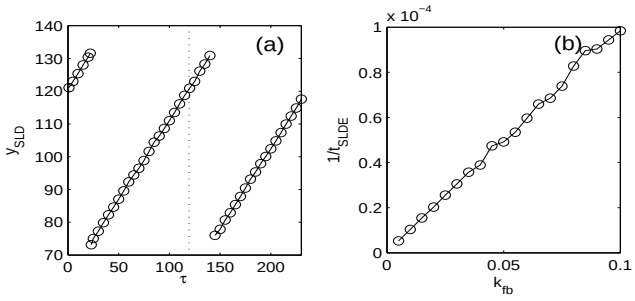

Fig. 3: (a) Location y_{SLD} of the SLD trajectory vs. time delay τ, where $k_{fb} = 0.05$. (b) $1/t_{SLDE}$ vs. the feedback gain k_{fb}, where t_{SLDE} is the time of the SLD ending over and inversely proportional to the drift velocity, $\tau = 10$.

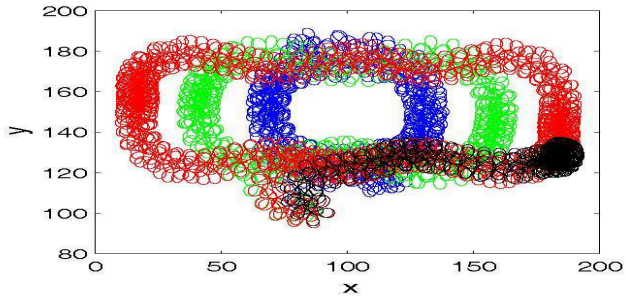

Fig. 4: (Color online) Trajectories of a spiral wave tip subjected to the feedback control for different lengths, L, of the line with the fixed location, $y_{fb} = 150$. L =40, 100, 160 and 180 for the blue, green, red and black lines. Here the center of the measuring lines is fixed at $(100, 150)$. $\tau = 10$, $k_{fb} = 0.05$.

Resonant drift of spiral wave under a straight-line feedback. – A single spiral can be induced from the equation system (1)-(2) without the feedback term by truncating a traveling pulse. The variables u and v are set initially to zero uniformly in the medium. To create a spiral wave, a super-threshold value $u = 0.8$ is given along a line near the boundary of the excitable medium to induce a propagating wave. When the propagating wave approaches the center of the excitable medium, one-half of the planar wave is erased by resetting $u = v = 0$. Subsequently, the open end of the planar wave curls into a spiral wave with its core located near the center of the excitable medium. The generated spiral wave rotates with a rotation period $T_0 \approx 0.58$ .t.u. (about 116 time steps) and a wavelength $\lambda \approx 5.8$ s.u. (about 58 space grids)(shown in Fig.1a). In the following parts of the paper, the units of time and space are time step and spatial grid, respectively.

Switching on the feedback control induces a drift of spiral wave core. In the system described by the equation (1) and (2), under a single point feedback, the spiral wave core has a drift along a stable circular orbits centered at the measuring point. The initial position of the detector with respect to the spiral tip, the time delay and the feedback gain make effects on the nature of the attractor, which is consistent with the feedback-controlled results from the open gel reactor and the Oregonator model[17-18]. Now we focus mainly on the resonant drift of spiral wave core subjected to a line feedback. Considering the long measuring line which is parallel to the x-axis and whose ends are on left and right boundaries, respectively, we find that the drift trajectory induced by the feedback signal is divided into three parts(shown in Fig.1 and Fig.2). In the part of trajectory labeled by 1 in Fig.2(a), the spiral wave core drift first outwards from the domain center to a certain location. In part 2 the trajectory starts a resonant drift from a certain location to the boundary along a straight line parallel to the measuring line, and finally stay near the boundary with the form of the complex meandering attractor in part 3. The final position of spiral core is close to either the left boundary or the right one, which is determined by the location y_{fb} of the measuring line. The straight line drift(SLD),which is defined as the part of the drift parallel to the measuring line and labeled by 2 in Fig.2(a), towards the right boundary occurs when $y_{fb} > 100$ and the SLD is towards the left boundary when $y_{fb} \leq 100$. In Figs.1(b) and 1(c) the movement directions of SLD mediated by the feedback derived from the line integral located at $y_{fb} = 150$ and $y_{fb} = 50$ are compared. From Fig.2 it is found that, when the absolute distance $|y_{fb} - 100|$ increases, the part of trajectory labeled by 1 rotates around the the initial spiral core in counter-clockwise direction. Fig.2 (d) shows also that, when $y_{fb} > 100$, the location y_{SLD} of the SLD part of the trajectory,which is computed by the arithmetic mean of the maximum and minimum y-values for the SLD part, is a piecewise linear-increasing function of y_{fb}. On each linear part the distance $y_{fb} - y_{SLD}$ has a constant value. The value for the left linear part is about 25, while it is about 82 for the right one.

The feedback is applied with a time delays τ. As can be seen in Fig.3(a), the value of τ affects the location y_{SLD} of SLD. The function $y_{SLD}(\tau)$ is T_0-periodic and piecewise linearly increasing. Further to increase or decrease the feedback gain k_{fb} does not result in a change in the drift trajectory of spiral core. However, it affects the drift velocity of the core. Fig.3(b) shows the relation between $1/t_{SLDE}$ and k_{fb}. t_{SLDE} is the time interval from the start of the drift to the formation of the final meandering attractor. It is inversely proportional to the drift velocity. $1/t_{SLDE}$ is nearly linearly rising with the increase of the k_{fb}. The effects of the length of the feedback line on a spiral wave are shown in Fig.4. When the line length L is significantly smaller than the spiral wavelength λ (about 58 space grids), the spiral core finally follows a circular path with the center of the short measuring line. The trajectories are similar to those for local feedbacks. When the length increases, the circular path is stretched along horizontal direction. If two ends of the line is close to left and right boundaries, respectively, a transient SLD and a final complex meandering attractor occurs.

Replacing the feedback line with several or dozens of

Fig. 5: (Color online) Trajectories(black) of a spiral wave tip under the double-line feedback for the different locations of the second measuring line. $y_{fb2} = 105$ in (a). $y_{fb2} = 140$ in (b). $y_{fb2} = 160$ in (c). $y_{fb2} = 165$ in (d). $y_{fb2} = 175$ in (e). $y_{fb2} = 185$ in (f). Here, the position of the first measuring line is fixed at $y_{fb1} = 150$, and $y_{fb2} > 100$. Red (green) curves show the trajectories when only the first(second) feedback line exists. $L_1 = 200$, $L_2 = 200$, $\tau = 10$ and $k_{fb} = 0.05$.

equi-spaced measuring points on the line, i.e., replacing the integral (4) with the sum $\frac{1}{N}\sum_{n=1}^{n=N} u(x'_n, y'_n, t)$, we observe the same drift trajectory as the line, where N is the total number of the measuring points. Fig.1(d) shows the trajectory of the spiral tip with a six-points feedback, where the points lie collectively on the line locating at $y_{fb} = 150$ and have an equi-spaced distribution from the left boundary to the right one. In this case, the spiral tip follows the trajectory including a SLD toward left boundary and a complex meandering attractor, which is nearly the same as the one shown in Fig.1(b). It has become widely accepted that the most dangerous cardiac arrhythmias are due to spiral waves or reentrant waves. Therefore,it is very important to control spiral waves in those systems. The above information tells that the feedback signal derived from several or dozens of measuring points can move the spiral core to the desired location along a chosen direction.

Resonant drift of spiral wave under a double-line feedback. – The effects of the double-line feedback on a spiral wave are examined by systematically varying the distance between two parallel measuring lines, as shown in Fig.5 and Fig.6. Suppose that the lines are parallel to $x-$axis, whose locations are described by y_{fb1} and y_{fb2}, respectively. In the simulations we fix $y_{fb1} = 150$ and change y_{fb2}. Figure 5 shows six typical examples of spiral tip trajectories found for different values of y_{fb2} under the condition $y_{fb2} > 100$. When the position y_{fb2} approaches to 100, the first part of the trajectory with double-line feedback is similar to the corresponding one of $y_{fb} = y_{fb1}$ in the single-line feedback. Because the drift velocity with a single-line feedback for y_{fb} near 100 is much smaller than that for y_{fb} far away from 100. After the transient period the trajectory forms directly a meandering attractor and doesn't undergo a SLD, as shown in Fig.5a. When $y_{fb2} > 130$, the SLD part appears in the trajectory. A consecutive increase of y_{fb2} results in a rotation in counter-clockwise direction for the first of the drift and a periodic variety of the SLD location. Because the same change occurs under a single-line feedback. A special case is observed for $y_{fb2} = 175$ due to the symmetry of singe-feedback trajectories for $y_{fb} = 150$ and for $y_{fb} = 175$, where the trajectory forms a meandering attractor near the initial core after undergoing a transitional circular drift(see Fig.5e). $y_{fb2} = 175$ is also a transition position in comparing the SLD location under the double-line feedback with that under the single-line feedback $y_{fb} = y_{fb2}$.

Fig. 6: (Color online) Similar to Fig.5, but here $y_{fb2} \leq 100$. $y_{fb2} = 5$ in (a). $y_{fb2} = 15$ in (b). $y_{fb2} = 30$ in (c). $y_{fb2} = 60$ in (d). $y_{fb2} = 65$ in (e). $y_{fb2} = 90$ in (f).

Now we examine the drift behavior under a double-line feedback with $y_{fb2} \leq 100$. When the second feedback line is close to the bottom boundary, the first part of the trajectory with the double-line feedback approaches that for the case with only the second line. See Figs.6(a) and 6(b). Because the drift velocity is large when the feedback line is close to the upper or lower boundary in the single-line feedback control. On the other hand, for a large y_{fb2} being close to 100, there is a first part approaching that of the single-line feedback $y_{fb} = 150$, see Fig.6(f). The reason is due to the small drift velocity when y_{fb} is close to 100. For moderate y_{fb2}, the drift includes the first part, whose location lies between the corresponding part of the single-line feedback $y_{fb} = y_{fb1}$ and that of $y_{fb} = y_{fb2}$, the long or short SLD, and the final meandering, see Figs.6(c)-(e). The SLD towards the left or right depends on the competition between the trajectories with the single-line feedback $y_{fb} = y_{fb1}$ and with $y_{fb} = y_{fb2}$.

Resonant drift of spiral wave under a contour-line feedback. – The role of domain shape has been studied in relation to reaction-diffusion systems with global feedback. Square-, circular-, triangular- and elliptical-shaped domains are commonly used in experiments and computations as they are simplest two-dimensional confined geometries. In this section the influence of contour-line of the feedback domains on the evolution of spiral waves is investigated in detail.

Figure 7 shows the drift trajectories that correspond to four square-shape contour lines with different side-lengths and a fixed center (140,100). When the side-length d is significantly smaller than the spiral wavelength λ, the spiral leaves the initial center by drifting toward the left until it turns to follow a circular path, as shown in Fig.7(a). This motion resembles those observed in the reported results applying a point feedback. In this case, when d increases, the radius of the resonance attractor becomes larger slowly. Around $d = 30$, the motion is changed, where the spiral core first drifts away from the initial core, then, it approaches a stable square trajectory, which is rotated by about 45°, see Fig.7(b). As a result of the significant increase of d, the spiral core is attracted toward a stable squared-trajectory with a large side-length and an orientation coinciding with the feedback contour, as shown in Fig.7(c). In the range where this kind of attractors create, the size of the square trajectory is slowly reduced with the increasing of d. An interesting cross-shaped trajectory is generated when increasing the contour-line size to $d = 90$. This trajectory can be considered as a combination of four small pieces of square trajectories linked together. With a further increase of d to make the left

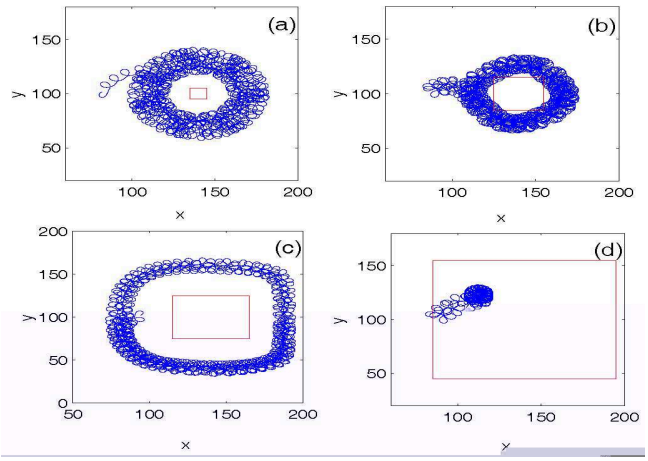

Fig. 7: (Color online) Trajectories of a spiral wave tip under various sizes of the square contour. Side length $d = 10$ in (a). $d = 30$ in (b). $d = 50$ in (c). $d = 110$ in (d). The contours are indicated by squares. $\tau = 10$, $k_{fb} = 0.05$.

side of the contour-line approach the initial core, a final complex meandering trajectory locates inside the contour, see Fig7.(d).

Keep the center of contour at $(90, 100)$ close to that of the initial spiral $(88, 100)$, we observe the trajectories of spiral wave tip under various side-lengths d of the square contour. As d increases, the trajectory is similar to the contours with the center at $(140, 100)$. The difference is that, after the stable square trajectory with orientational angle 45° with respect to the feedback contour, the complex meandering attractor locating at the initial core appears.

Discussion and conclusion. – The analysis of spiral wave dynamics under feedback control via a line may be performed via the drift velocity mediated by the corresponding feedback. Here the dynamics can be understood via the results of one-point feedback.

When $k_{fb} > 0$, the drift induced by feedback can be expressed as[32]

$$\gamma(x, y) = \varphi + \omega\tau + \phi(x, y) \tag{5}$$

where (x, y) is the Cartesian coordinates of the core center of spiral unperturbed spiral wave, ω is the fundamental frequency in the Fourier expansion of the feedback signal. When a one-point feedback is applied, the phase of feedback signal follows

$$\phi(x, y) = \pi + arctan(\frac{y}{x}) + \frac{2\pi}{\lambda}\sqrt{x^2 + y^2} \tag{6}$$

for any points (x, y) except the measuring point $(0, 0)$. The drift velocity field is obtained from the phase $\phi(x, y)$ and Eq.(5). The domain center is a stable fixed point, since within its vicinity drift vectors are oriented toward the origin. A radial displacement of the core center is accompanied by a counterclockwise rotation of the vectors. At a certain displacement the vectors are orientated perpendicularly to the radial direction. It turns out that the circle with certain radius is a limiting cycle of the drift velocity field. The limiting cycle represents the so-called resonance attractor of spiral wave.

Let us assume that the drift of spiral core is mainly affected by the points which are in the feedback line and are the nearest from the core center. The spiral first leaves the position where its core was initially placed by drifting until it reaches the circular attractor of these points. After traveling a short distance, the neighboring points start to become the new nearest points. The spiral core turns to follow the attractor of the neighboring points, which may be obtained by translating the former attractor. This process is continued until the spiral core reaches the vicinity of boundary, and the SLD part being parallel to the feedback line forms. When the tip approaches the boundary, the feedback signal is periodic because the feedback line crosses with the spiral wave, as shown in Fig.1. So the complex meandering attractor is generated in the domain close to the boundary. Replacing the feedback line with several or dozens of equi-spaced measuring points on the line, the same drift trajectories are observed. It may be explained by the similarities between the attractor of one-point feedback and that of the short-line feedback with the length significantly smaller than the spiral wavelength.

Based on the above explanations, the distance $|y_{SLD} - y_{yb}|$ corresponds to the radius R of the resonance attractor under one-point feedback, which can be obtained from Ref.[32] to be

$$\frac{R}{\lambda} = m - 0.25sign(k_{fb}) - \frac{\varphi}{2\pi} - \frac{\tau}{T_\infty} \tag{7}$$

where m is an integer. By transforming y_{SLD} to $|y_{SLD-}y_{yb}|$, it is easy to find that Figs.2(d) and 3(a) agree qualitatively with the theoretical predictions given by Eq.(7). For each value of τ there are several possible stable attractors corresponding to different values of the integer m, which results in the piecewise behavior of drift lines versus feedback lines and time delay.

In this letter,we discussed also the dynamics of spiral wave under the double-line feedback and square-shaped contour one. The trajectory of spiral tip with the double-line feedback may be understood via the competition between two corresponding single-line feedbacks. A variety of attractors can be obtained from a contour-line feedback.

* * *

This work is supported by the National Natural Science Foundation of China [under Grant Nos.10647127 and 10775018], Science Foundations of Hebei Education Department[under Grant No.2009135], Hebei Nature Science Foundation Project[under Grant No. A2006000128] and Science Foundation Of Hebei Normal University.

REFERENCES

[1] Cross M C. and Hohenberg P C., *Rev. Mod. Phys.*, **65** (1993) 852.
[2] Courtemanche M, *Chaos.*, **6** (1996) 579.
[3] Nettesheim S.,Oertzen A V.,Rotermund H H. and Ertl G., *J. Chem. Phys.*, **98** (1993) 9977.
[4] Frisch T.,Rica S.,Coullet P. and Gilli J M., *Phys. Rev.Lett.*, **72** (1994) 1471.
[5] Frisch C A.,Panfilov A V.,Hogeweg P.,Siegert F and Weijer C J., *J.theor.Biol.*, **181** (1996) 203.
[6] Winfree A T. and Strogatz S H., *Physca.D*, **8** (1983) 35.
[7] Gray R A.,Jalife J.,Panfilov A V.,Baxter W T.,Cabo C.,Davidenko J M. and Pertsov A.M., *Science*, **270** (1995) 1222.
[8] Huang X.,Troy W C.,Yang Q.,Ma H.,Schiff S J., and Wu J Y., *J.Neuroscience*, **24** (2004) 9897.
[9] Kim M., Bertram M., Pollmann M., Oertzen A., Mikhailov A S., Rotermund H H. and Ertl G., *Science*, **292** (2001) 1357.
[10] Sakaguchi H. and Fujimoto T., *Phys. Rev. E*, **67** (2003) 067202.
[11] Wang P Y. and Xie P., *Phys. Rev. E*, **61** (2000) 5120.
[12] Zhang H., Cao Z., Wu N J., Ying H P. and Hu G., *Phys. Rev. Lett.*, **94** (2005) 188301.
[13] Yuan G Y.,Wang G R. and Chen S G., *Europhys.Lett.*, **72** (2005) 908.
[14] Yuan G Y., Chen S G. and Yang S P., *Eur.Phys.J.B*, **58** (2007) 331.
[15] Steinbock O.,Zykov V S. and Müller S C., *Nature*, **366** (1993) 322.
[16] Grill S., Zykov V S. and Müller S C., *J. Phys. Chem.*, **100** (1996) 19082.
[17] Braune M. and Engel H., *Phys. Rev. E.*, **62** (2000) 5986.
[18] Grill S., Zykov V S. and Müller S C., *Phys. Rev. Lett .*, **75** (1995) 3368.
[19] Karma A and Zykov V S., *Phys. Rev. Lett .*, **83** (1999) 2453.
[20] Zykov V S., Kheowan O U., Rangsiman O. and Müller S C., *Phys. Rev. E.*, **65** (2002) 026206.
[21] Kheowan O U., Zykov V S., Rangsiman O. and Müller S C., *Phys. Rev. Lett .*, **86** (2001) 2170.
[22] Goldschmidt D M., Zykov V S. and Müller S C., *Phys. Rev. Lett .*, **80** (1998) 5220.
[23] Zykov V S., Brandtstädter H.,Bordiougov G. and Engel H., *Phys. Rev. E.*, **72** (2005) 065201R.
[24] Zykov V S., Bordiougov G., Brandtstädter H., Gerdes I. and Engel H., *Phys. Rev. Lett.*, **92** (2004) 018304.
[25] Zykov V S. and Engel H., *Phys. Rev. E.*, **70** (2004) 016201.
[26] Zykov V S., Mikhailov A S. and Müller S C., *Phys. Rev. Lett.*, **78** (1997) 3398.
[27] Kheowan O U., Zykov V S. and Müller S C., *Phys. Chem. Chem. Phys.*, **4** (2002) 1334.
[28] Kheowan O U., Kantrasiri S., Wilairat P., Storb U. and Müller S C., *Phys. Rev. E.*, **70** (2004) 046221.
[29] Kheowan O U., Kantrasiri S.,Uthaisar ., Gáspár V. and Müller S C., *Chem.Phys.Lett.*, **389** (2004) 140.
[30] Kheowan O U., Chan C K., Zykov V S., Rangsiman O. and Müller S C., *Phys. Rev. E.*, **64** (2001) 035201.
[31] Naknaimueang S., Allen M A. and Müller S C., *Phys. Rev. E.*, **74** (2006) 066209.
[32] Zykov V S. and Engel H., *Physica D.*, **199** (2004) 243.
[33] FitzHugh R., et al, *Biophys. J.*, **1** (1996) 445.
[34] Courtemanche M., Skaggs W. and Winfree A T., *Physica D.*, **41** (1990) 173.

This figure "Fig5.jpg" is available in "jpg" format from:

http://arxiv.org/ps/1004.0045v1

This figure "Fig6.jpg" is available in "jpg" format from:

http://arxiv.org/ps/1004.0045v1